Support Information

Enhanced High-Strength, Temperature-Resistant PVA Hydrogel Sensors with Silica/Xanthan/Glycerol for Posture Monitoring and Handwriting Recognition Using Deep Learning

Fanchen Luo [a], Yafei Qin *, [a], Xi Wang [a], Xuanmo Zhao [a], Kedi Chen [a], Weichen Huang [a]

[a] Faculty of Mechanical and Electrical Engineering, Kunming University of Science and technology, Kunming 650500, China.

* E-mail: qinyafei_kmust@foxmail.com

Table S1 statistics of mechanical properties of hydrogels with different compositions

Sample code	Elongation at break	Tensile strength	Young's Modulus	Toughness (MJ/m^3)
PVA	268	0.527	0.57	0.61
PL	378	0.416	0.61	0.63
PLX	438	0.604	0.98	1.109
PLXS	611	0.943	1.12	2.37
PLXSG	796	1.816	1.768	6.09

Table S2 Statistics on the mechanical properties of hydrogels at different silica concentrations

Sample code	Elongation at break	Tensile strength	Young's Modulus	Toughness (MJ/m^3)
$PLXSG_0$	414	0.813	1.815	1.80
$PLXSG_1$	689	1.163	1.392	4.53
$PLXSG_5$	796	1.817	1.768	6.09
$PLXSG_{10}$	612	2.610	4.336	8.579

Table S3 Statistics of mechanical properties of PLXSG hydrogels at different temperatures

Temperature (°C)	**Elongation at break**	**Tensile strength**	**Young's Modulus**	**Toughness (MJ/m^3)**
-40	918	1.235	1.268	5.69
0	807	1.688	1.615	6.01
25	796	1.817	1.768	6.09
70	625	4.219	7.56	8.83

Table S4 Comparison of the performance of PLXSG hydrogel with reported hydrogel flexible strain sensors

Hydrogel	Conductivity (S/cm)	Stress (MPa)	GF
PVA/SBMA/2HEMA	0.0458	0.376	3.356
PAAm/c-PAAm	0.0114	0.142	1.24
PAM/SA/MXene/sucrose	0.0087	0.082	1.768
PVA/GA /PANi	0.0017	0.693	2.5
MP/FeCl3	0.15	1.5	2.02
PAAm/FH	0.0668	0.099	2.06
This work	0.768	1.8	3.623

Table S5 Comparison of the performance of PLXSG hydrogel with reported conductive materials for strain sensing

Material	GF	Stress (MPa)	Strain (%)	Available temperature range (°C)	Ref.
Graphene/Silicone rubber	>143	6.92	465	/	1
Pmc/CS/f-Fe_3O_4-Fe^{3+}	1.75	2.33	1158	/	2
PA/CS/ Gly / MXene	3.93	0.12	918	-20 — 80	3
Silane modified MXene/CNF	/	~ 0.06	120	-20 — 200	4
PEDOT：PSS/PDMS foam	Piezoresistive 6.25	~ 0.04	Compressive strain ~ 60	25-100	5
PAM/QACNF/MXene	2.24	0.449	1706	/	6
PVA/Li^+/Xan/SiO_2/Gly	3.623	1.8	796	-40 — 80	This work

CS denotes chitosan, Gly denotes glycerol, Pmc and PA denote poly (acrylamide-co-acrylic acid), CNF denotes cellulose nanofiber, PEDOT: PSS denotes poly(3,4-ethylenedioxythiophene)-poly (styrene sulfonate), PDMS denotes polydimethylsiloxane, PAM denotes polyacrylamide, and QA denotes quaternate.

Table S6 Composition of PL_XXSG hydrogel.

<table>
<tr><th>PVA(g)</th><th>LiCl(g)</th><th>Xan(g)</th><th>SiO_2</th><th>Gly(g)</th><th>DL(g)</th></tr>
<tr><td rowspan="5">1</td><td>0</td><td rowspan="5">0.052</td><td rowspan="5">5wt% solution</td><td>3.6</td><td>3.6</td></tr>
<tr><td>0.293</td><td>3.45</td><td>3.45</td></tr>
<tr><td>0.586</td><td>3.31</td><td>3.31</td></tr>
<tr><td>0.879</td><td>3.16</td><td>3.16</td></tr>
<tr><td>1.172</td><td>3.01</td><td>3.01</td></tr>
</table>

Table S7 Composition of PLX_XSG hydrogel.

<table>
<tr><th>PVA(g)</th><th>LiCl(g)</th><th>Xan(g)</th><th>SiO_2</th><th>Gly(g)</th><th>DL(g)</th></tr>
<tr><td rowspan="4">1</td><td rowspan="4">0.586</td><td rowspan="4">0.052</td><td>0wt% solution</td><td rowspan="4">3.31</td><td rowspan="4">3.31</td></tr>
<tr><td>1wt% solution</td></tr>
<tr><td>5wt% solution</td></tr>
<tr><td>10wt% solution</td></tr>
</table>

Table S8 Composition of P、PL、PLX、PLXS and PLXSG.

PVA(g)	LiCl(g)	Xan(g)	SiO_2	Gly(g)	DL(g)
1	0	0	0wt% solution	0	7.61
1	0.607	0	0wt% solution	0	7.01
1	0.588	0.052	0wt% solution	0	6.97
1	0.586	0.052	5wt% solution	0	6.62
1	0.586	0.052	5wt% solution	3.31	3.31

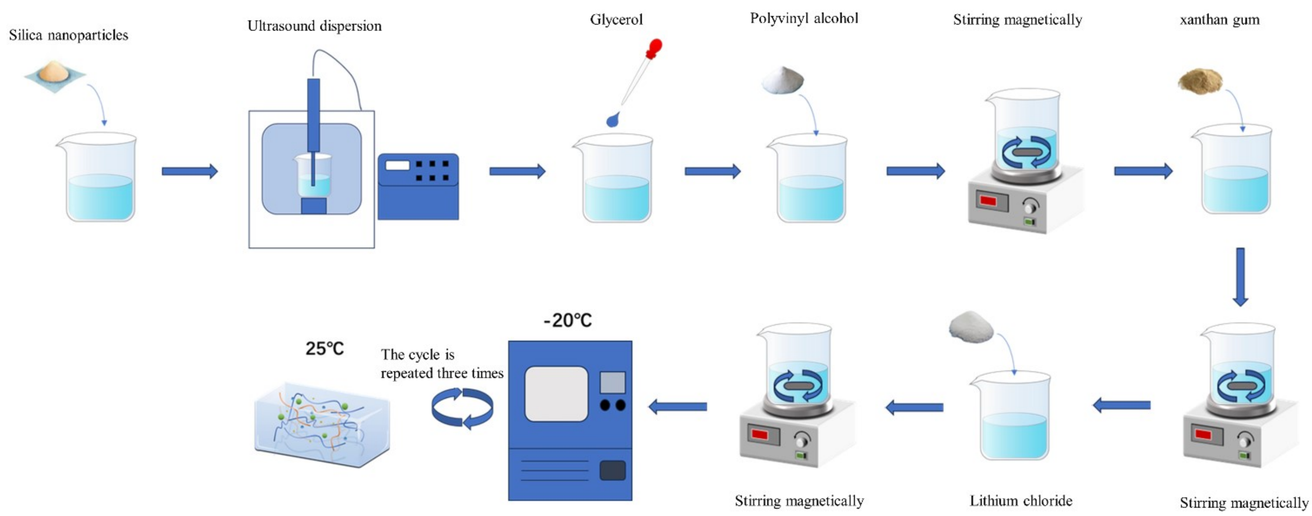

Figure S1 PLXSG hydrogel preparation process

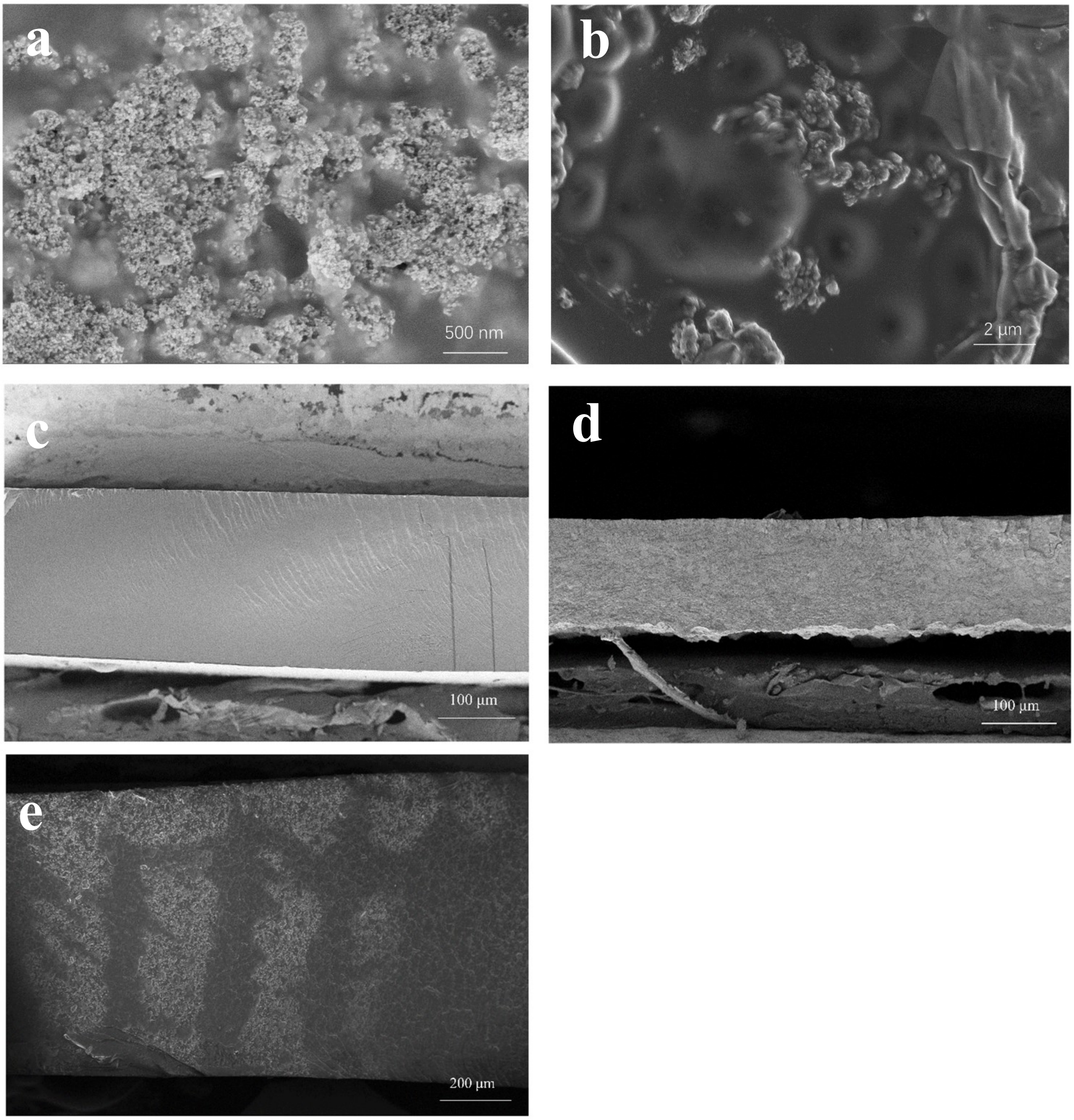

Figure S2 (a) SEM image of PLXS hydrogel at 500 nm scale. **(b)** SEM image of PLXSG hydrogel at 2 μm scale. **(c)** SEM image of cross section of PL hydrogel at 100 μm scale. **(d)** Cross-sectional SEM image of PLXS hydrogel at 100 μm scale. **(e)** Cross-sectional SEM image of PLXSG hydrogel at 200 μm scale.

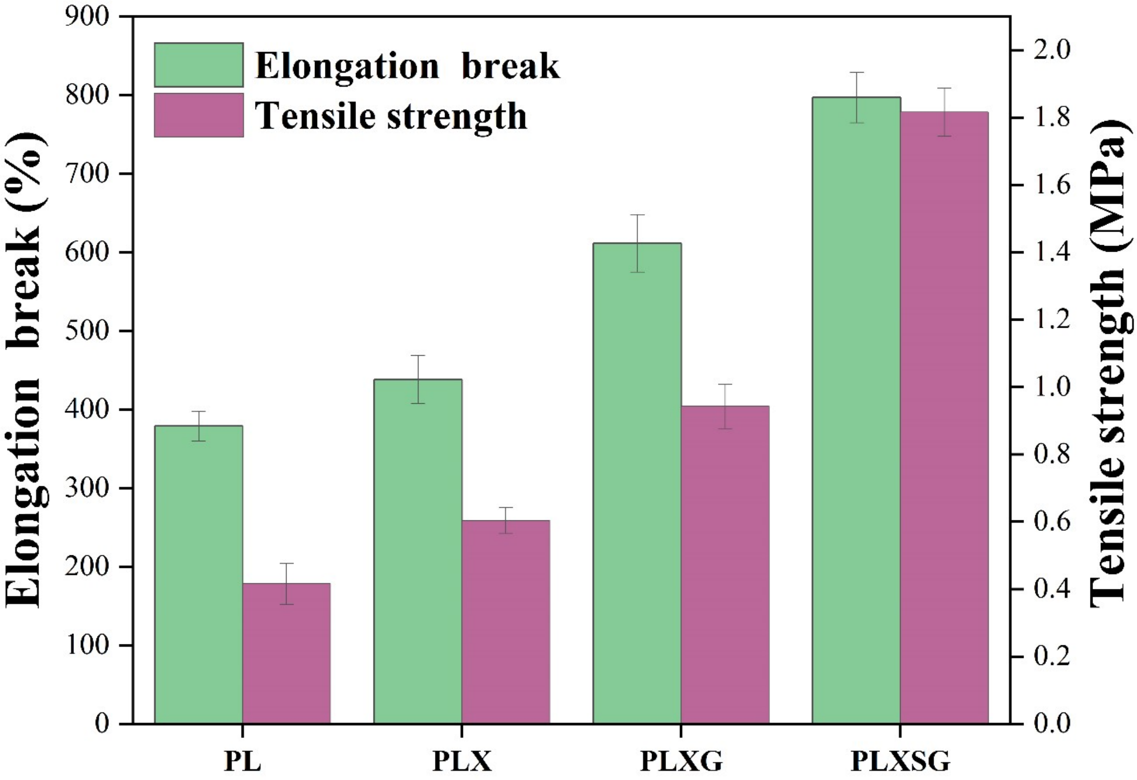

Figure S3 Maximum strain and maximum stress of hydrogels with different fractions.

The data indicates that as xanthan, silica, and glycerol are incrementally added, there is a corresponding gradual increase in both the maximum extensibility and the maximum stress of the hydrogels. This suggests a positive enhancement of the hydrogels' mechanical properties by each additive.

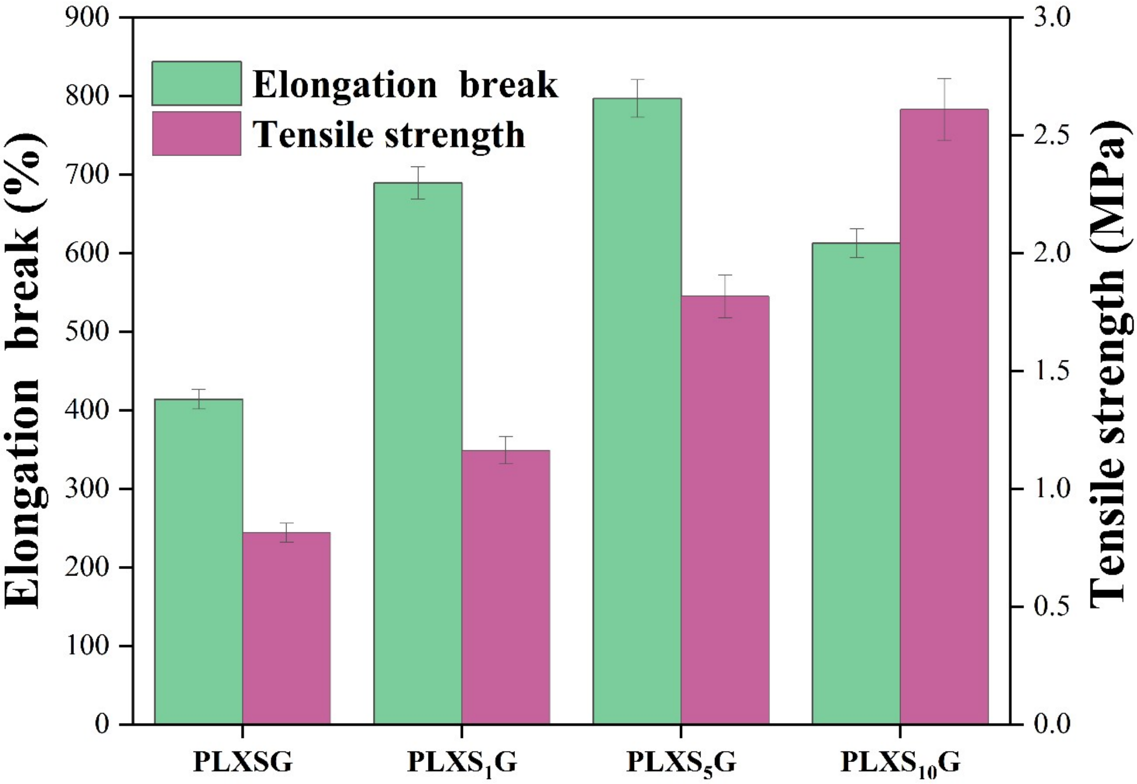

Figure S4 Maximum strain and maximum stress of hydrogels with different silica concentrations.

As the concentration of silica rises, the tensile ratio of the hydrogel initially increases and then decreases, whereas the tensile strength consistently correlates with the increasing concentration.

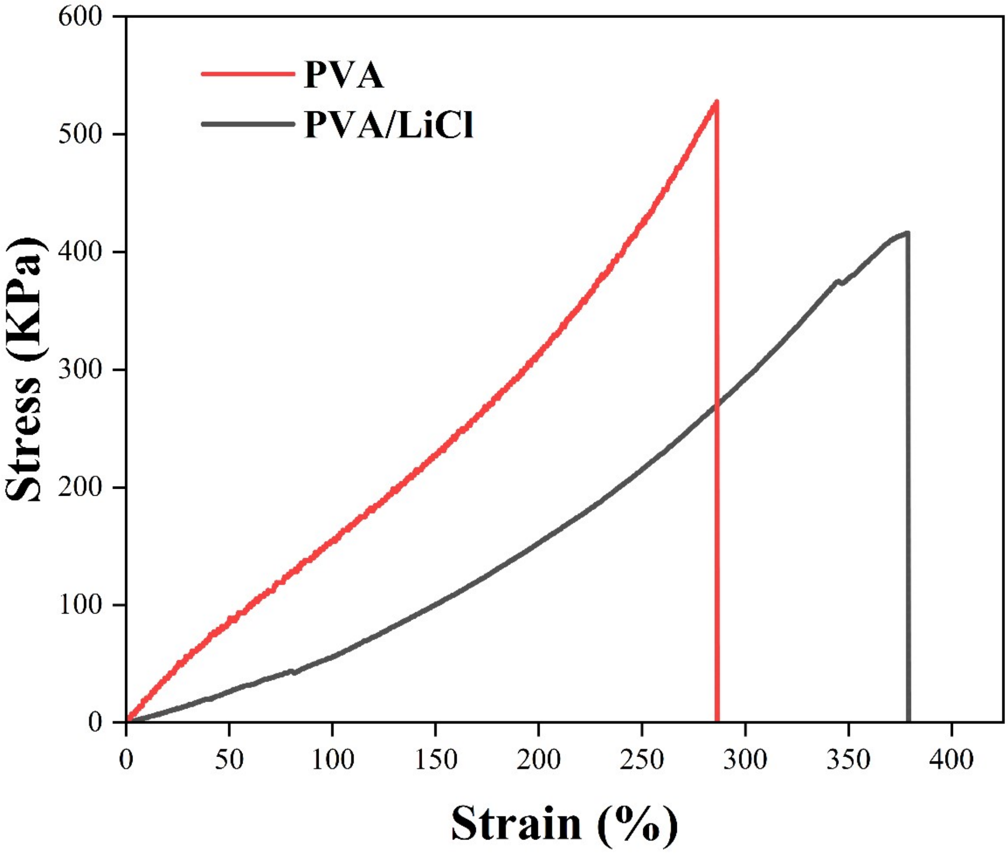

Figure S5 Stress-strain curves of PVA and PVA/LiCl hydrogels.

The PVA/LiCl hydrogel exhibited improved tensile properties over the PVA hydrogel; however, its mechanical strength decreased from 0.527 MPa to 0.416 MPa.

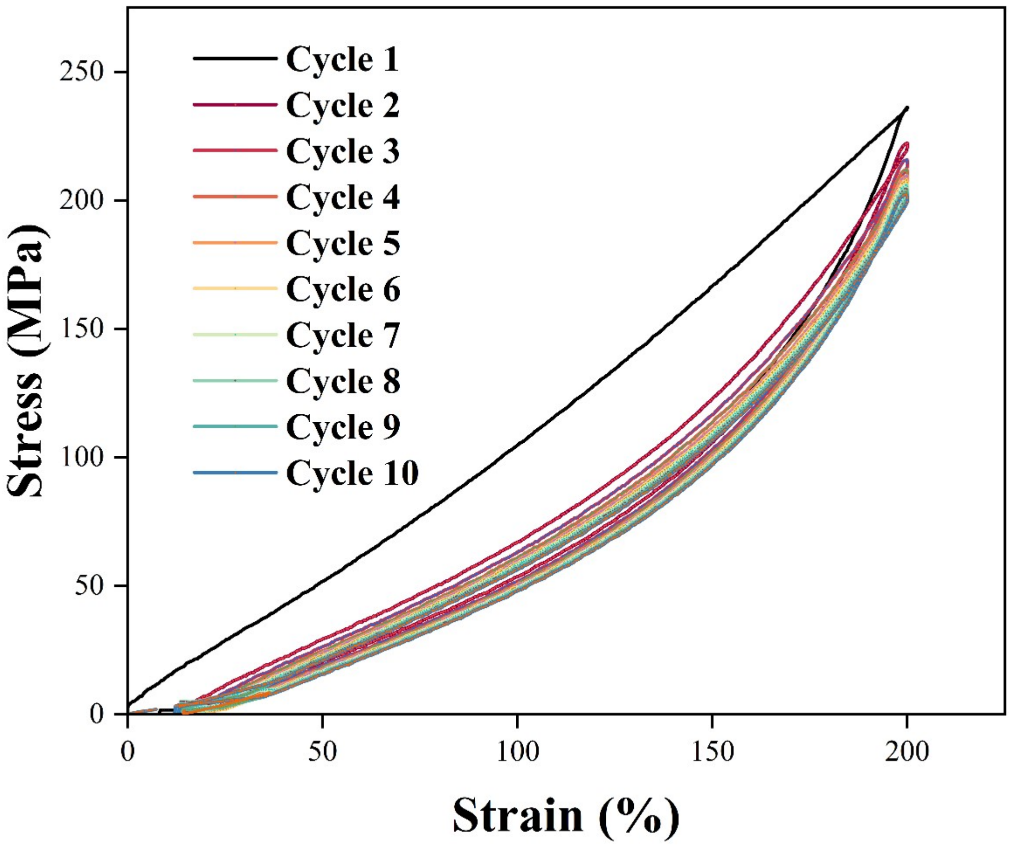

Figure S6 Cyclic tensile stress-strain curves of PLXSG hydrogels at 200% of maximum strain.

The PLXSG hydrogel demonstrated superior hysteresis performance through 10 cycles of 200% tensile strain, evident from the reduced hysteresis area depicted in Fig. S6.

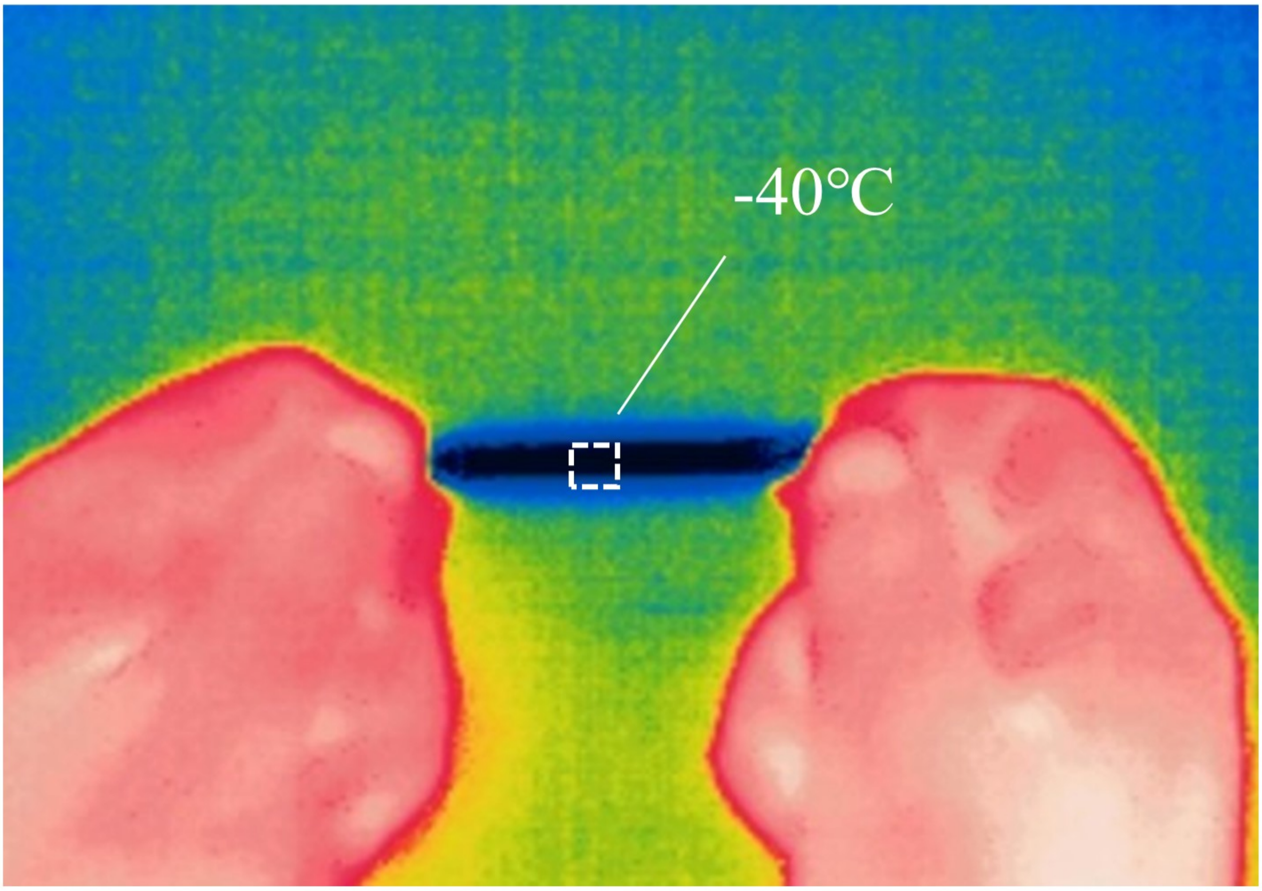

Figure S7 Infrared thermography of PLXSG hydrogel stretched at -40°C

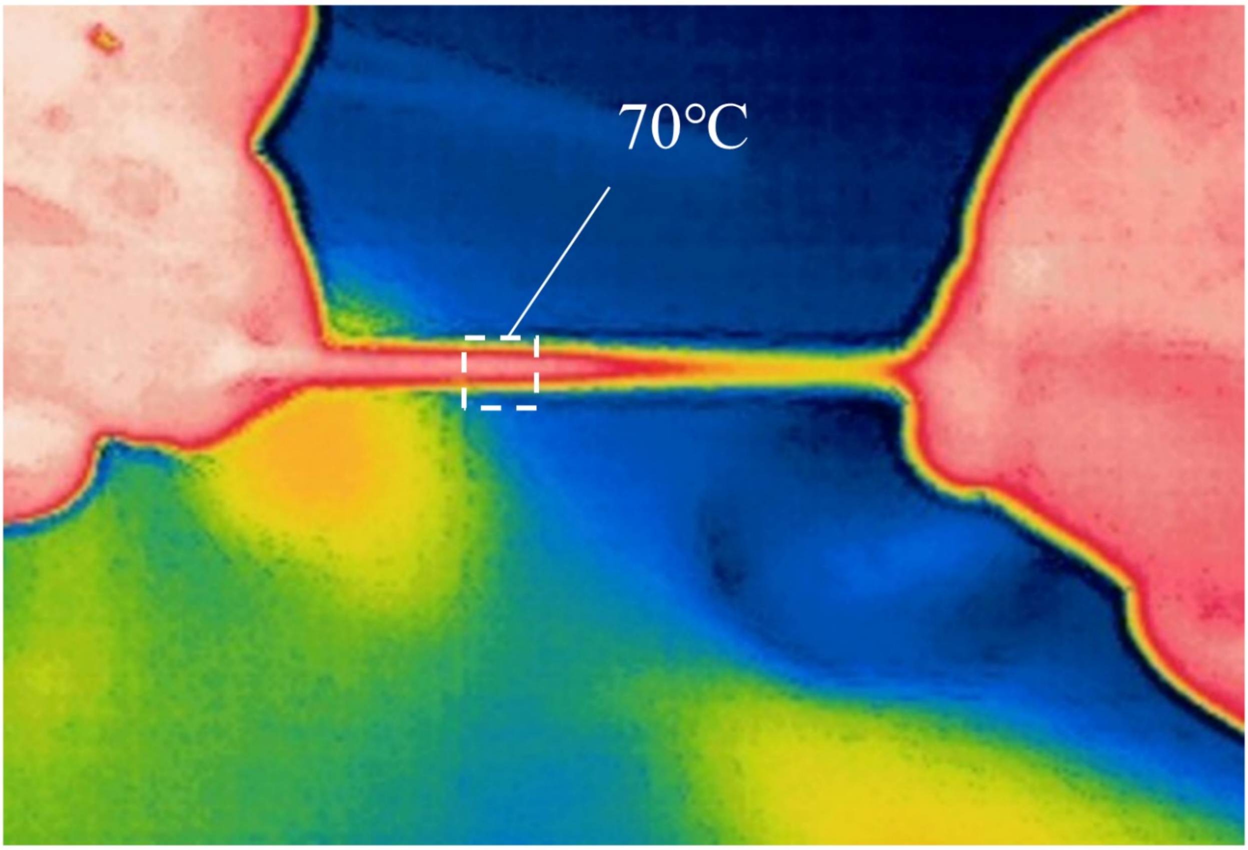

Figure S8 Infrared thermogram of PLXSG hydrogel stretched at 70°C

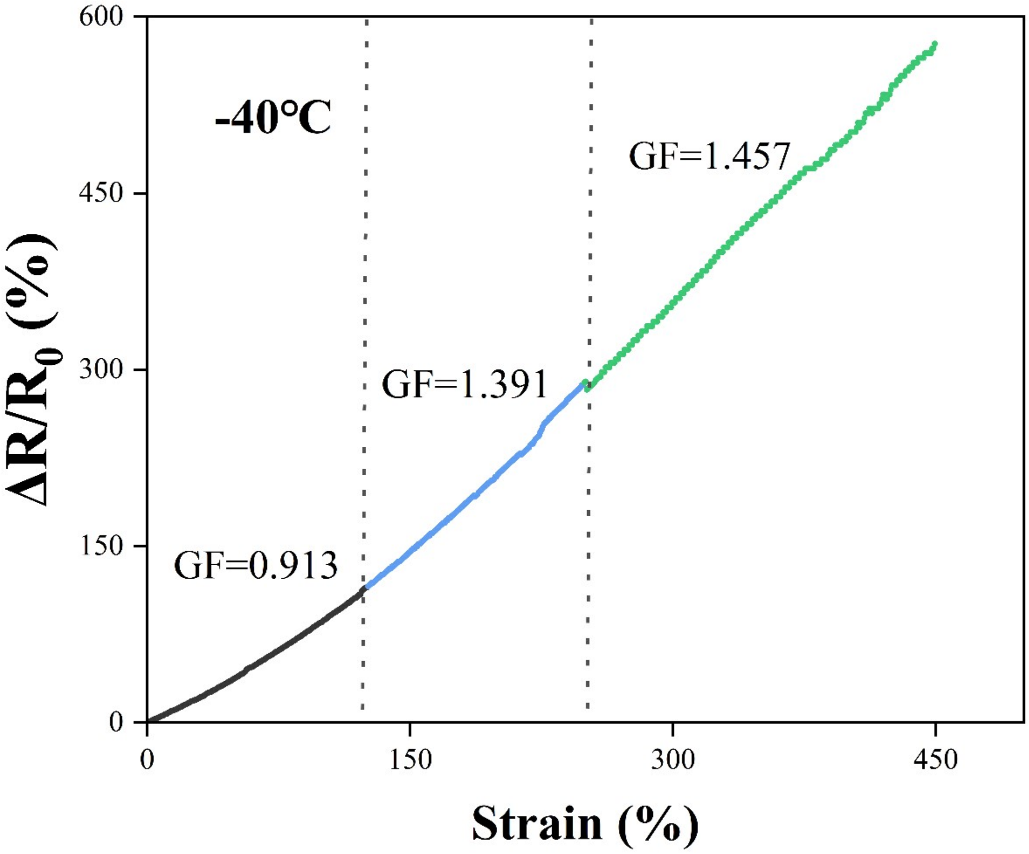

Figure S9 PLXSG hydrogel as strain sensor GF at -40°C.

At 70°C, the PLXSG hydrogel exhibits a gauge factor (GF) of 1.283 for strains above 320% and a GF of 0.565 for strains below 180%, as shown in Figure S9.

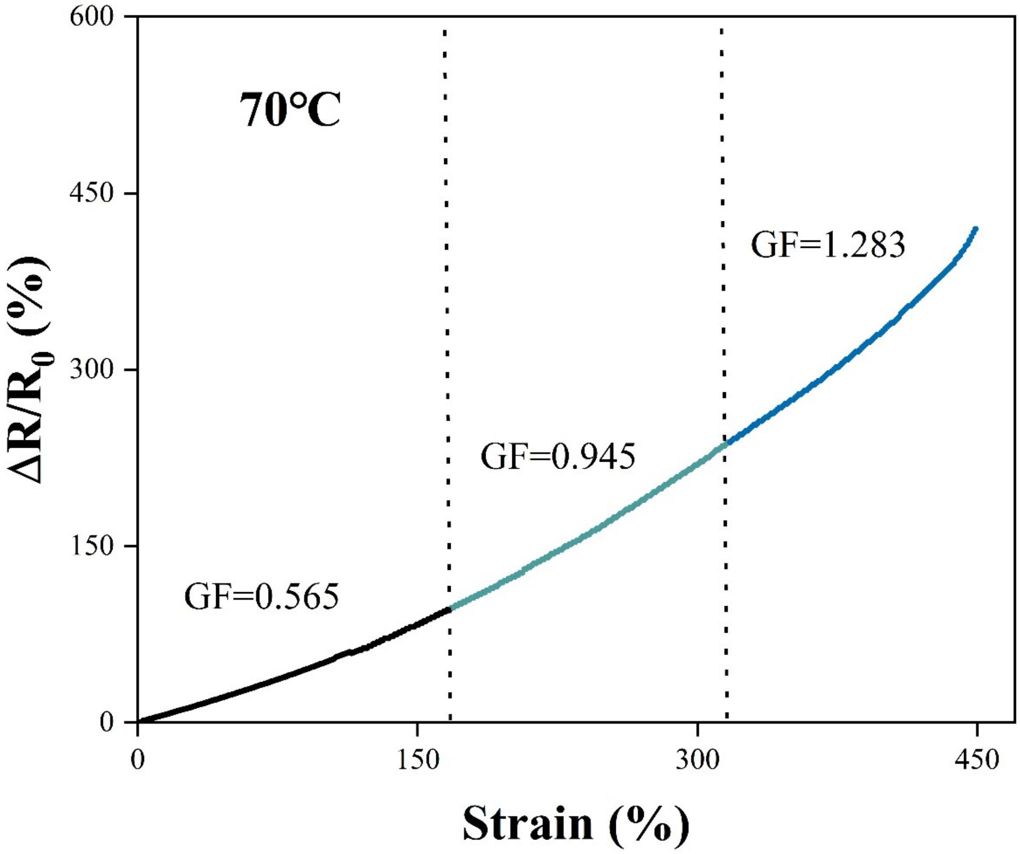

Figure S10 PLXSG hydrogel as strain sensor GF at 70°C.

At -40°C, the GF is 1.457 for strains above 270% and 0.913 for strains below 130%. Despite the significant reduction in GF at extreme temperatures compared to room temperature, the hydrogel remains functional as a strain sensor.

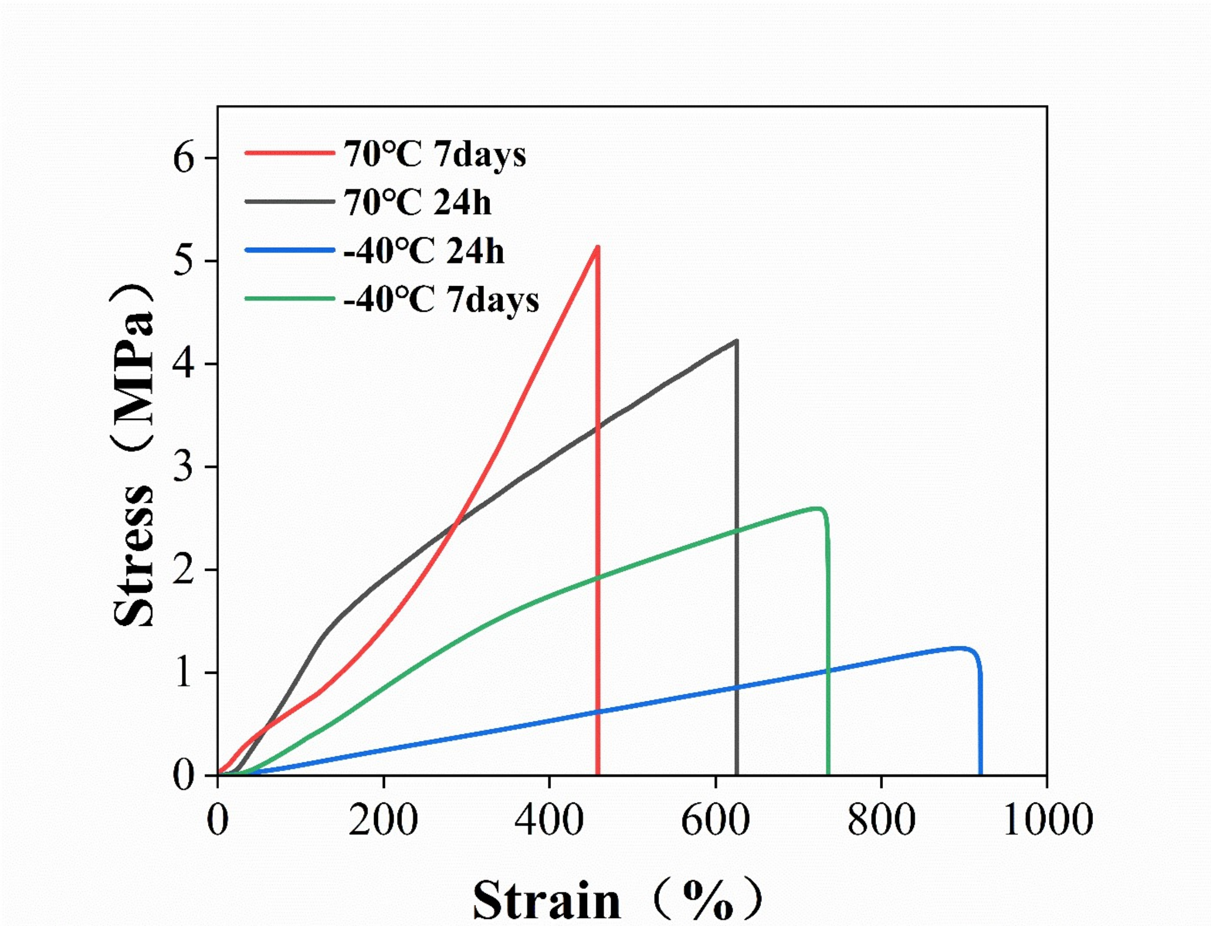

Figure S11 The stress-strain curves of PLXSG hydrogels were analyzed after being placed at 70°C and -40°C for 24 hours and 7 days.

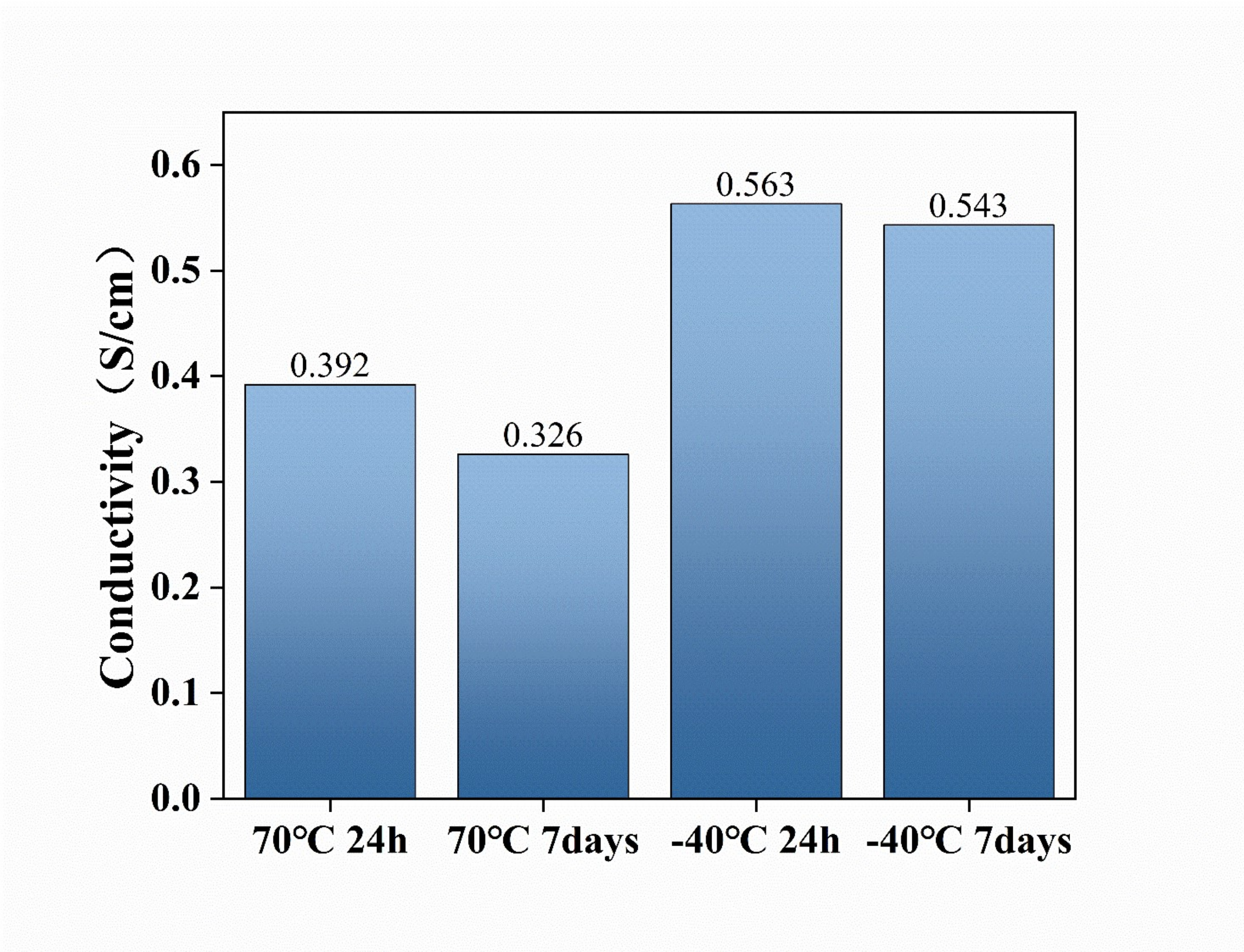

Figure S12 Comparison of the conductivity of PLXSG hydrogels after 24 hours and 7 days at 70°C and -40°C.

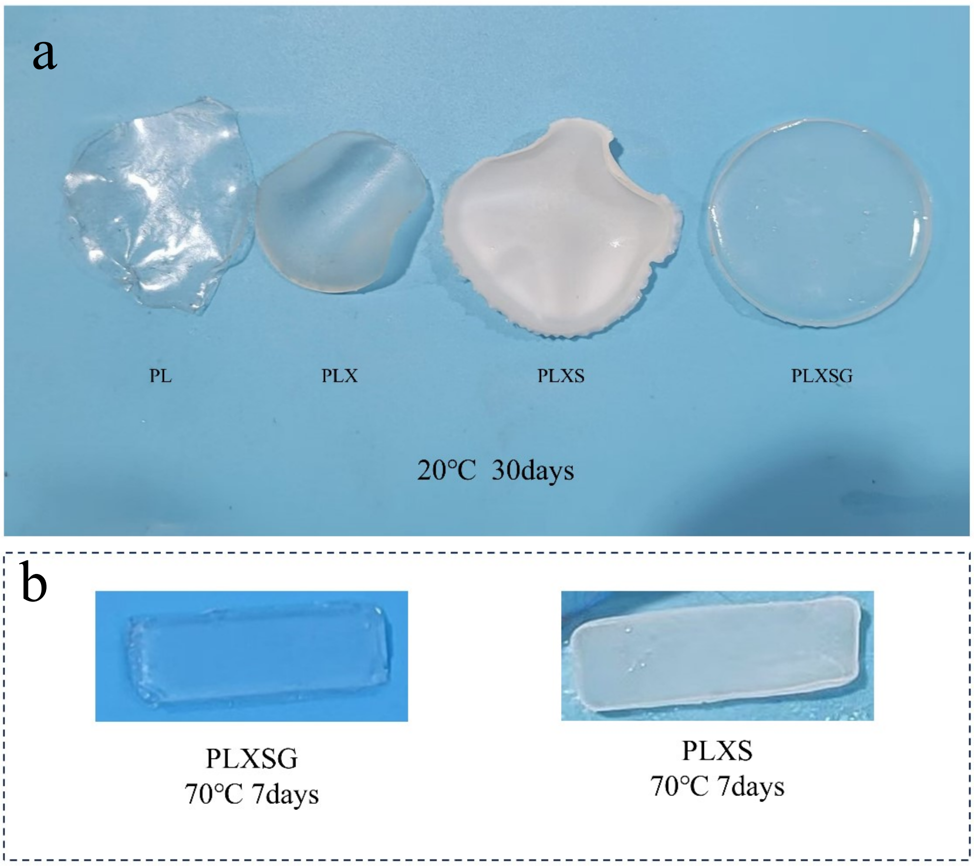

Figure S13 a Photographs of PL, PLX, PLXS, and PLXSG hydrogels after 30 days at 20°C. **Figure S13 b** Photographs of PLXSG and PLXS hydrogels after 7 days at 70°C.

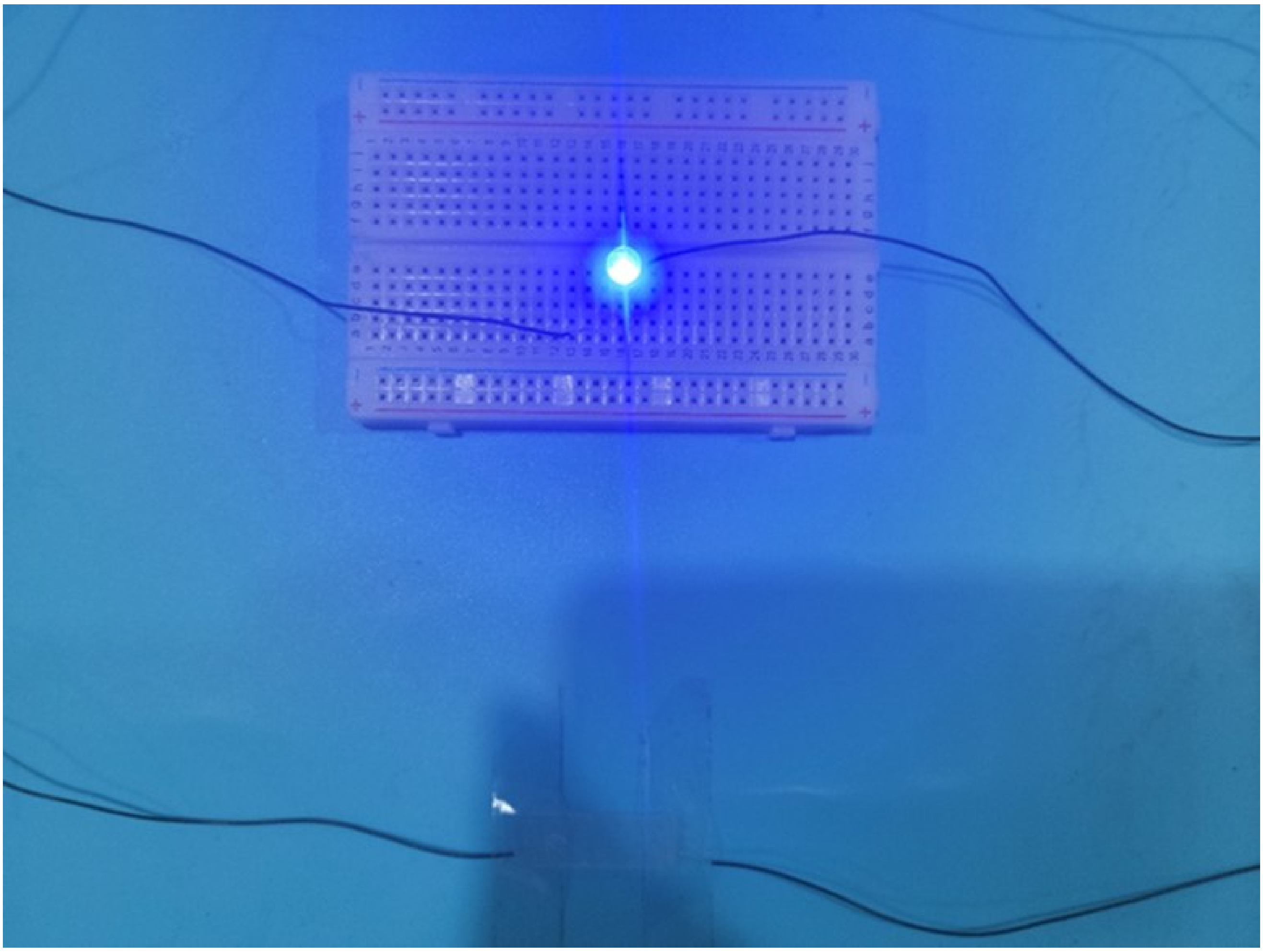

Figure S14 PLXSG hydrogel illuminates LEDs at -40°C

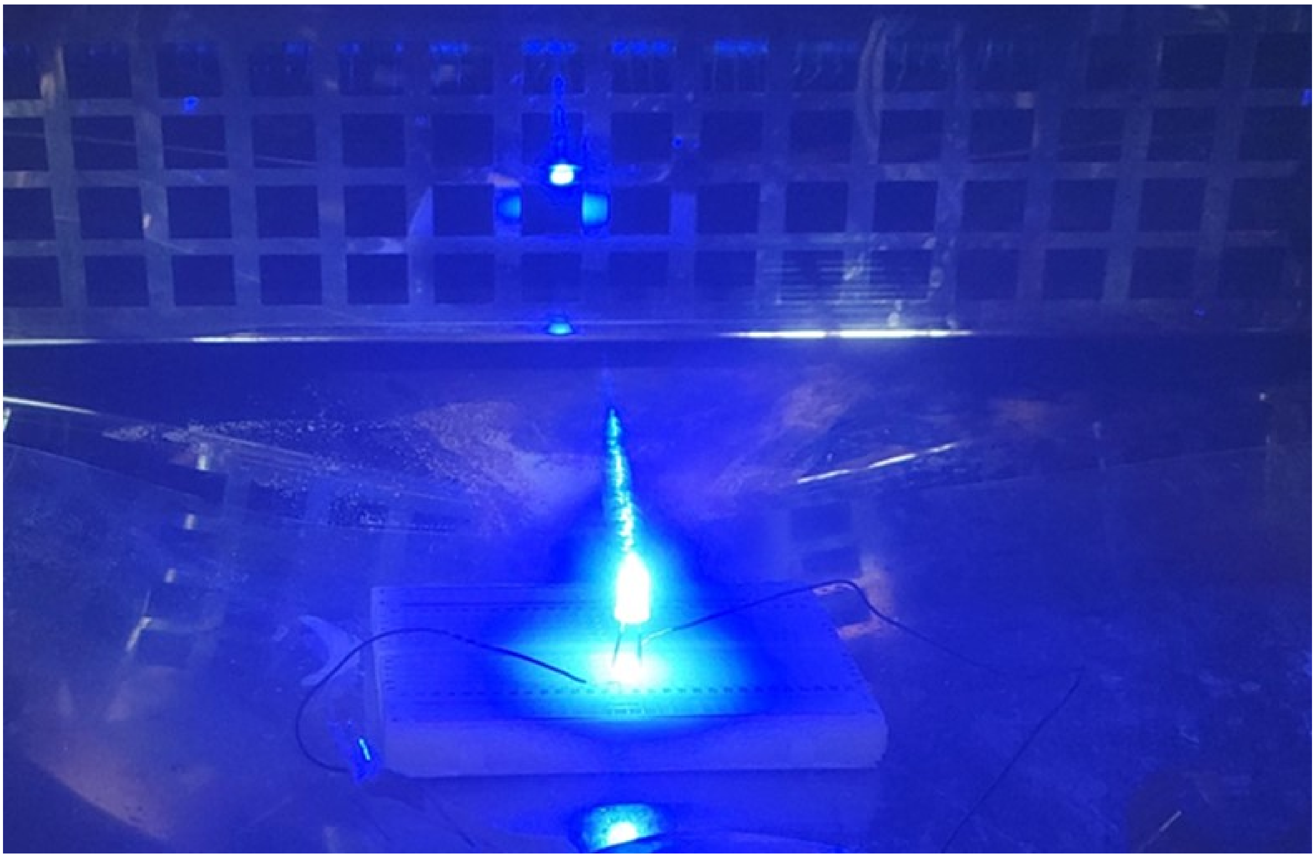

Figure S15 PLXSG hydrogel illuminates LEDs at 70°C

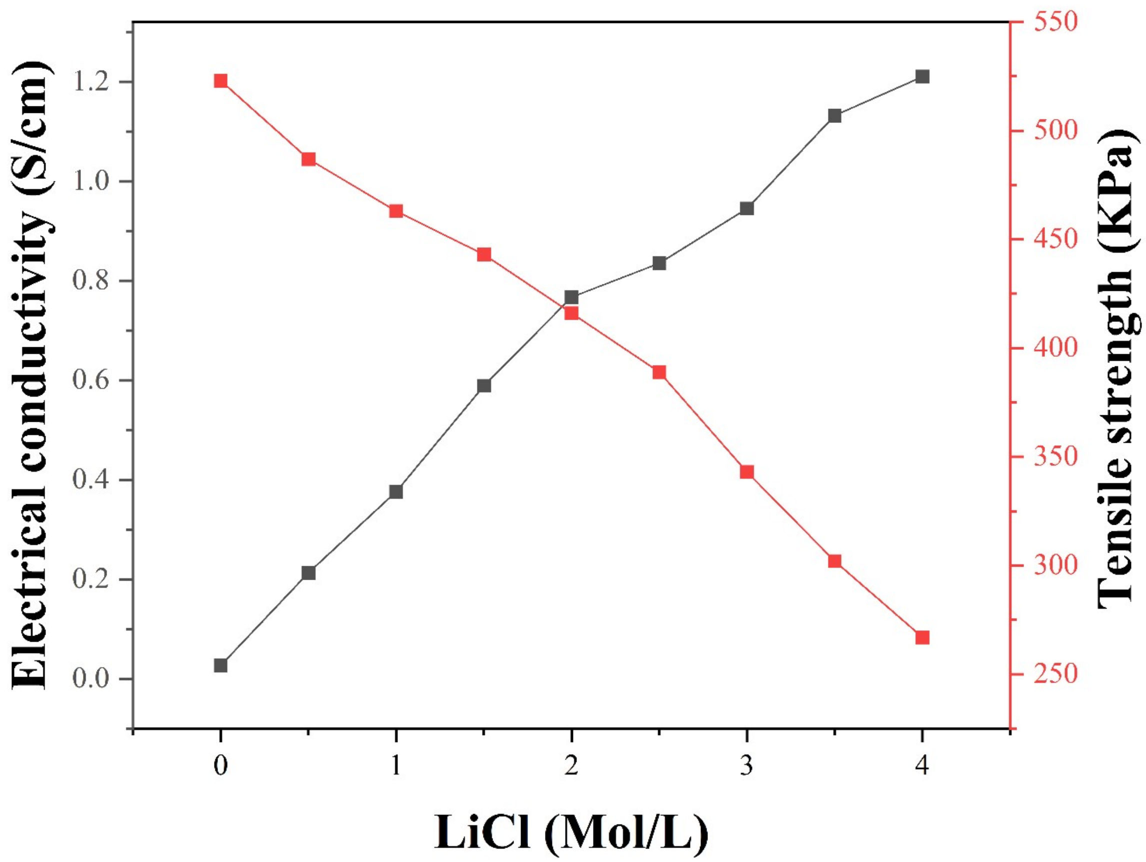

Figure S16 Conductivity and tensile strength of hydrogels with different lithium chloride concentrations.

As the lithium chloride concentration increases, there is a corresponding gradual increase in hydrogel conductivity and a decrease in tensile strength. An optimal balance between these properties is attained at a 2 M concentration.

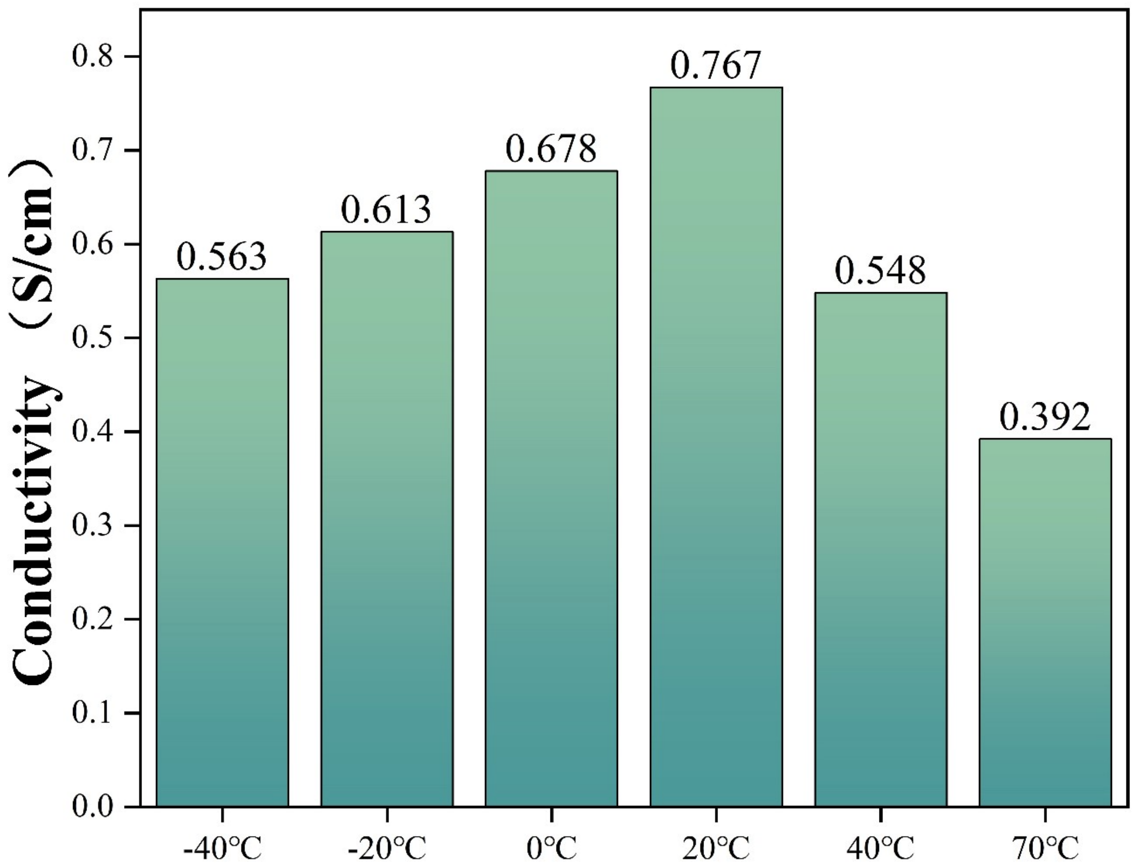

Figure S17 Change in conductivity of hydrogels at different temperatures.

The conductivity of PLXSG hydrogels significantly drops as the temperature rises, halving at 70 degrees Celsius compared to room temperature. Additionally, conductivity diminishes slowly at lower temperatures, but the decline is more gradual than at higher temperatures.

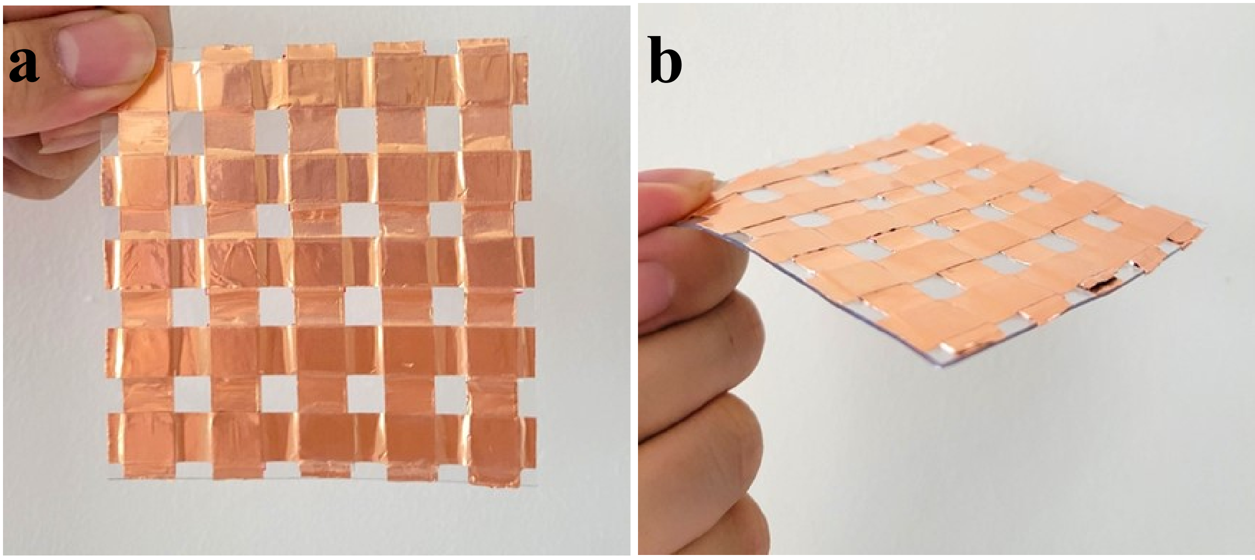

Figure S18 hydrogel sensor array.

1 H. Yang, X. Yao, Z. Zheng, L. Gong, L. Yuan, Y. Yuan and Y. Liu, Compos Sci Technol, 2018, 167, 371–378.

2 S.-N. Li, B. Li, Z.-R. Yu, L.-X. Gong, Q.-Q. Xia, Y. Feng, D. Jia, Y. Zhou and L.-C. Tang, Compos Sci Technol, 2020, 195, 108173.

3 S.-N. Li, Z.-R. Yu, B.-F. Guo, K.-Y. Guo, Y. Li, L.-X. Gong, L. Zhao, J. Bae and L.-C. Tang, Nano Energy, 2021, 90, 106502.

4 H.-Y. Chen, Z.-Y. Chen, M. Mao, Y.-Y. Wu, F. Yang, L.-X. Gong, L. Zhao, C.-F. Cao, P. Song, J.-F. Gao, G.-D. Zhang, Y.-Q. Shi, K. Cao and L.-C. Tang, Adv Funct Mater, 2023, 33, 2304927.

5 F. Nie, Y.-L. Gu, L. Zhao, L.-T. Li, F.-X. Shen, J. Song, J. Liu, G.-D. Zhang, J.-F. Gao, P. Song, Y. Shi and L.-C. Tang, Advanced Sensor Research, 2024, 3, 2300140.

6 Q.-Y. Ni, X.-F. He, J.-L. Zhou, Y.-Q. Yang, Z.-F. Zeng, P.-F. Mao, Y.-H. Luo, J.-M. Xu, B. Jiang, Q. Wu, B. Wang, Y.-Q. Qin, L.-X. Gong, L.-C. Tang and S.-N. Li, J Mater Sci Technol, 2024, 191, 181–191.